Environ Sci Pollut Res (2014) 21:12279–12293
DOI 10.1007/s11356-014-3135-x

RESEARCH ARTICLE

A reactive transport model for mercury fate in soil—application to different anthropogenic pollution sources

Bertrand Leterme · Philippe Blanc · Diederik Jacques

Received: 5 November 2013 / Accepted: 30 May 2014 / Published online: 15 June 2014

Abstract Soil systems are a common receptor of anthropogenic mercury (Hg) contamination. Soils play an important role in the containment or dispersion of pollution to surface water, groundwater or the atmosphere. A one-dimensional model for simulating Hg fate and transport for variably saturated and transient flow conditions is presented. The model is developed using the HP1 code, which couples HYDRUS-1D for the water flow and solute transport to PHREEQC for geochemical reactions. The main processes included are Hg aqueous speciation and complexation, sorption to soil organic matter, dissolution of cinnabar and liquid Hg, and Hg reduction and volatilization. Processes such as atmospheric wet and dry deposition, vegetation litter fall and uptake are neglected because they are less relevant in the case of high Hg concentrations resulting from anthropogenic activities. A test case is presented, assuming a hypothetical sandy soil profile and a simulation time frame of 50 years of daily atmospheric inputs. Mercury fate and transport are simulated for three different sources of Hg (cinnabar, residual liquid mercury or aqueous mercuric chloride), as well as for combinations of these sources. Results are presented and discussed with focus on Hg volatilization to the atmosphere, Hg leaching at the bottom of the soil profile and the remaining Hg in or below the initially contaminated soil layer. In the test case, Hg volatilization was negligible because the reduction of Hg^{2+} to Hg^0 was inhibited by the low concentration of dissolved Hg. Hg leaching was mainly caused by complexation of Hg^{2+} with thiol groups of dissolved organic matter, because in the geochemical model used, this reaction only had a higher equilibrium constant than the sorption reactions. Immobilization of Hg in the initially polluted horizon was enhanced by Hg^{2+} sorption onto humic and fulvic acids (which are more abundant than thiols). Potential benefits of the model for risk management and remediation of contaminated sites are discussed.

Keywords Mercury · Hg · Reactive transport modelling · HP1 · Geochemical speciation · Vadose zone · Leaching

Responsible editor: Michael Matthies

Electronic supplementary material The online version of this article (doi:10.1007/s11356-014-3135-x) contains supplementary material, which is available to authorized users.

B. Leterme (✉) · D. Jacques
Performance Assessments, Institute for Environment, Health, and Safety, Belgian Nuclear Research Centre (SCK•CEN), Boeretang 200, 2400 Mol, Belgium
e-mail: bleterme@sckcen.be

P. Blanc
D3E/BGE, Bureau de Recherches Géologiques et Minières (BRGM), Av. C. Guillemin 3, BP6009, 45060 Orleans, France

Introduction

Historical production of mercury (Hg) and associated contamination of the environment started more than 500 years ago, but industrial and related usages of Hg increased markedly in the twentieth century (Hylander and Meili 2003). This led to numerous sites of important soil contamination, posing significant threats to human health and ecosystem quality (see Ottesen et al. 2013 for an overview of hot spots of anthropogenic contamination sites in Europe). Recent investigations indicated that release from contaminated sites was very important with respect to the global Hg balance (Driscoll et al. 2013; Kocman et al. 2013).

For soil systems in particular, Hg pollution can result from direct contamination (spilling, landfill, mine tailings, etc.) or from indirect pathways such as the deposition of prior atmospheric emissions (Guédron et al. 2013). The main anthropogenic sources of soil contamination identified are Hg mining, gold and silver mining, manufacturing (chlor-alkali plants, manometer spill), wood preservation and cemeteries (through

the release of Hg from dental amalgams) (UNEP 2002). This variety of Hg release forms and phases means that speciation in contaminated areas is often complex to apprehend (Bloom et al. 2003), as it may vary over short distances (e.g. Millan et al. 2011) and be influenced by co-contaminants (Renneberg and Dudas 2001). Aging since the time of contamination is also of importance because phase transformations or retention mechanisms can show relatively slow kinetics (Davis et al. 1997; Biester et al. 1999).

The characterization of Hg contamination in soils has considerably improved over the last decade following developments in mercury speciation analysis techniques (Andrews 2006; Li et al. 2012). For instance, quantifying Hg complexation with dissolved organic matter (DOM) is nowadays better addressed using X-ray absorption spectroscopy. As a consequence, field surveys of Hg contamination currently go beyond the measurement of "total amount of Hg" and provide detailed information on Hg speciation (Bernaus et al. 2006; Navarro et al. 2006; Santoro et al. 2010). In parallel, the understanding of Hg biogeochemistry in soils is continuously improving (Skyllberg 2012). However, simulation tools are missing for using this data at the scale of a contaminated site and for modelling Hg fate in the unsaturated zone under variably saturated and transient flow conditions. More specifically, geochemical reactions such as aqueous speciation or specific sorption to functional groups on soil organic matter are seldom explicitly taken into account when modelling the migration and fate of Hg in soil systems. Studies on mercury transport in the unsaturated zone usually focus on the topsoil and gaseous Hg emission or transport (e.g. Navarro-Flores et al. 2000; Zhang et al. 2002; Walvoord et al. 2008) but do not include any chemical reactions (i.e. gaseous Hg is assumed to behave conservatively). To our knowledge, the only study of reactive transport modelling of Hg in the unsaturated zone was by Bessinger and Marks (2010), who investigated a site of historical mercury fulminate ($Hg(CNO)_2$) production and numerically tested remediation by adjunction of activated carbon. A reason for the relative lack of Hg geochemical modelling studies in unsaturated soils may be the difficulty to fully characterize these systems in order to exploit the capabilities of reactive transport models (Steefel et al. 2005). This problem was illustrated by Shaw et al. (2006), who simulated Hg and CN^- leaching in PHREEQC assuming saturated conditions even though their experiments were conducted under unsaturated conditions. Alternatively, simplified models exist for simulating Hg transport in soils, but they do not include geochemical reactions. For example, in models simulating Hg fluxes between different "pools" (atmosphere, soils, rivers and sediments…), Hg leaching is often calculated using empirical equations (Tipping et al. 2011; Futter et al. 2012). As far as saturated media are concerned, recent applications of reactive transport modelling of Hg include Bessinger et al. (2012), Zhu et al. (2012) and Johannesson and Neumann (2013).

The objective of the present study is to develop a model capable of simulating Hg fate and transport in unsaturated soil systems including effects of variably saturated water flow, specifically addressing anthropogenic sources of contamination. In a first part, the conceptual model is presented and the main equations implemented in the HP1 numerical code (Jacques et al. 2006, 2008a, b) are given. Then a set of hypothetical test cases using different contamination sources (elemental, solid and aqueous Hg) and combinations hereof are presented. The results are discussed on the basis of indicators such as Hg leaching or the amount of Hg that is sorbed to the soil organic matter. Finally, the potential contributions of the model to pollution risk assessment and remediation are discussed.

Development of a model of Hg fate in soil systems

Conceptual model

Figure 1a shows the mercury cycle from the perspective of soil systems. Sources of Hg (both anthropogenic and natural) include ore deposits, the atmosphere, vegetation and human activities. Vegetation and the atmosphere can also be considered as Hg sinks for soil systems, together with surface and ground water. Figure 1a furthermore includes the main chemical and transport processes affecting Hg fate in soil systems. Not all these processes are considered relevant for the development of our conceptual model, as its scope is limited to the pollution resulting from human activities that lead to a direct input into soil systems (spills, mining, etc.). Therefore, atmospheric wet and dry depositions are ignored. The resulting Hg flux to soil systems coming from these is generally very small compared to that from other anthropogenic activities. For the same reason, vegetation uptake and litter fall are not considered in the model. Plant root uptake of Hg from soils is generally very low and can be neglected (Schuster 1991; Pant et al. 2010) even though exceptions exist (e.g. Pérez-Sanz et al. 2012). The migration of Hg as a non-aqueous-phase liquid (NAPL) is not considered as it appears to be negligible in non-cracked soils (Eichholz et al. 1988), but the dissolution of residual Hg NAPL is included as one of the possible sources of contamination to represent historical NAPL pollution. Finally, mercury methylation is not included because the present model assumes oxic conditions in which this process is less important (Ullrich et al. 2001; Skyllberg et al. 2003).

To summarize, the key processes and phase changes retained for the model are aqueous speciation and complexation (with organic and inorganic ligands), Hg sorption to solid organic matter (SOM) and desorption, leaching, Hg precipitation and dissolution, residual Hg NAPL dissolution, Hg^{2+} reduction to Hg^0 and volatilization (Fig. 1b).

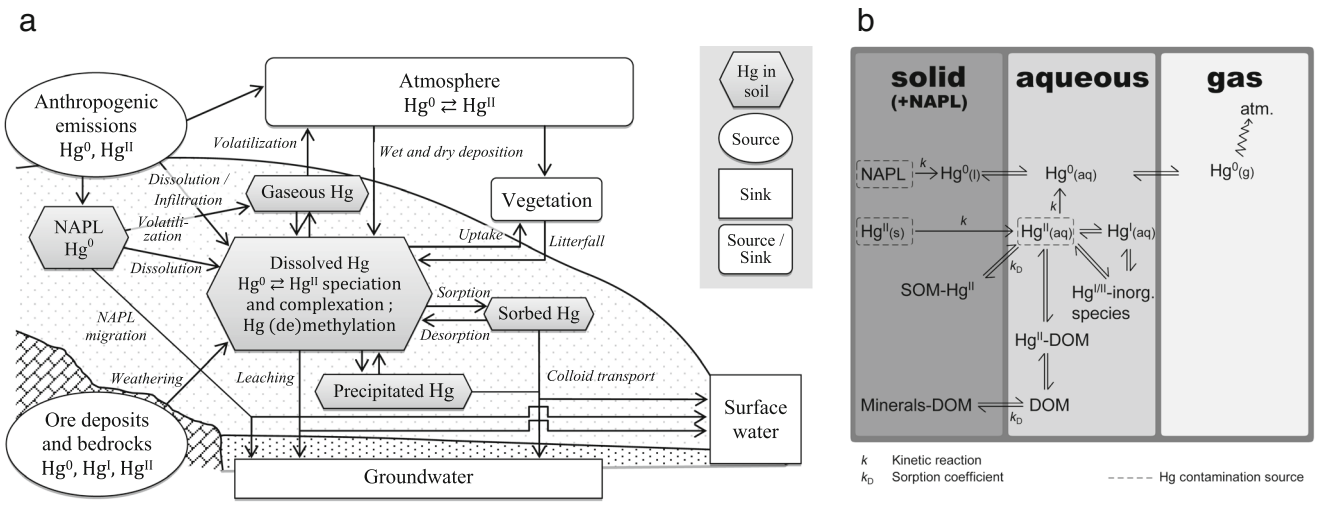

Fig. 1 **a** Mercury cycle in soil systems. *Oval shapes* denote Hg sources, *rectangles* are for Hg sinks and *rounded rectangles* are components that can act as both sources and sinks. **b** Conceptual model of Hg speciation and reactions in the solid, aqueous and gas phases. Initial Hg release can be in the form of NAPL, solid or aqueous phase

Mathematical model

The mathematical description of the conceptual model requires three types of equations: (i) Richards' equation for variably saturated water flow in soil systems; (ii) advective-dispersive or diffusive transport of the primary species in the aqueous and gaseous phases, respectively; and (iii) thermodynamic (equilibrium) and kinetic geochemical reactions, phase transformations and phase transfers (solid to aqueous phase and reverse transfers, as well as aqueous-gaseous exchange). The soil is conceptualized as a three-phase system at the continuum scale, and flow and transport processes are defined for a uniform porous medium. This section presents the full mathematical description of the model.

Water flow

The water flow equation is based on mass conservation within a given soil volume and on flux summation to and from this volume. Fluxes are described using the Darcy-Buckingham law relating the flux to the pressure head gradient in the variably saturated soil and a moisture-dependent proportionality factor. The resulting one-dimensional Richards equation for water flow in soils is given by Eq. 1:

$$\frac{\partial\theta(h)}{\partial t}=\frac{\partial}{\partial x}\left[K(h)\left(\frac{\partial h}{\partial x}+\cos\alpha\right)\right]-S(h) \tag{1}$$

where h is the soil water pressure head [L], θ the volumetric water content [$L^3\ L^{-3}$], t time [T], x the spatial coordinate [L] (positive upward), S the sink term to represent root water uptake [$L^3\ L^{-3}\ T^{-1}$], α the angle between the flow direction and the vertical axis, and K is the unsaturated hydraulic conductivity [$L\ T^{-1}$]. To describe the relations between θ–h and K–h, the van Genuchten equations (van Genuchten 1980) are used, as shown in Eqs. 2 and 3:

$$\theta(h)=\theta_r+\frac{\theta_s-\theta_r}{(1+|\alpha h|^n)^m} \tag{2}$$

and

$$K(h)=K_s S_e^l\left[1-\left(1-S_e^{1/m}\right)^m\right]^2 \tag{3}$$

where θ_r is the residual water content [$L^3\ L^{-3}$]; θ_s the saturated water content [$L^3\ L^{-3}$]; α [L^{-1}], n [−] and m (=1−1/n) [−] shape parameters; l a pore connectivity parameter [−]; K_s the saturated hydraulic conductivity [$L\ T^{-1}$]; and $S_e=(\theta-\theta_r)/(\theta_s-\theta_r)$ the effective saturation.

Solute movement

Solute transport is only calculated for so-called primary species for which the total concentration is defined as

$$C_j=c_j+\sum_{i=1}^{N_{sa}}\nu_{ji}c_i \tag{4}$$

where C_j is the total concentration of the primary species j [$M\ L^{-3}$], c_j the concentration of aqueous species j, c_i the concentration of the ith secondary aqueous species, ν_{ji} the stoichiometric coefficient of the primary species j in the ith secondary species and N_{sa} the number of secondary aqueous species. For a species-independent diffusion coefficient,

solute transport in the aqueous phase is described by the advective-dispersive equation:

$$\frac{\partial \theta C_j}{\partial t} = \frac{\partial}{\partial x}\left(\theta D^w \frac{\partial C_j}{\partial x}\right) - \frac{\partial q C_j}{\partial x} - S C_{r,j} + R_{o,j} \quad (5)$$

where S is the sink term in the water flow equation [L^3 L^{-3} T^{-1}], $C_{r,\,j}$ the total concentration of the sink term [M L^{-3}], D^w the dispersion coefficient in the liquid phase [L^2 T^{-1}] and $R_{o,\,j}$ the source/sink term that represents various heterogeneous equilibrium and kinetic reactions (e.g. cation exchange, surface complexation, mineral dissolution) and homogeneous kinetic reactions (e.g. degradation reactions in the aqueous phase) [M L^{-3} T^{-1}]. In the gaseous phase, diffusion is the only transport process:

$$\frac{\partial \theta_a C_j}{\partial t} = \frac{\partial}{\partial x}\left(\theta_a D^a \frac{\partial C_j}{\partial x}\right) + R_{o,j} \quad (6)$$

where θ_a is the air content [L^3 L^{-3}]. The dispersion coefficients D^w and D^a in Eqs. 5 and 6, respectively, are given by

$$\begin{aligned} \theta D_i^w &= D_L|q| + \theta D_{i,w}\tau_w \\ \theta_a D_i^a &= \theta_a D_{i,a}\tau_a \end{aligned} \quad (7)$$

where $D_{i,\,w}$ and $D_{i,\,a}$ [L^2 T^{-1}] are, respectively, the molecular diffusion of aqueous species i in free water and gaseous species i in the gas phase, D_L is the longitudinal dispersivity [L] and τ_w and τ_w [−] are the tortuosity factors in the liquid and gaseous phases, which are related to the water content by the model of Millington and Quirk (1961).

Aqueous speciation and complexation

Aqueous complexation reactions between inorganic and organic primary species are calculated using a thermodynamic approach (mass action laws) and the Debye-Hückel activity correction model. To do so, we use a version of the Thermoddem database (Blanc et al. 2012) updated for inorganic mercury species. The database was extended to surface complexation reactions by including specific equilibrium constants from Skyllberg (2012).

The selection of the Hg species is obtained from the following reliable sources: the CODATA database (Cox et al. 1989), the IUPAC (Powell et al. 2005), the Baes and Mesmer (1976) selection and a specific review by Bessinger and Apps (2005). The selection process is explained in more details in Online Resource 1. Only a limited refinement of thermodynamic properties was performed due to a lack of experimental data. Verification was achieved by drawing predominance diagrams and comparing with similar diagrams found in literature (see the example in Online Resource 1)

Complexation of Hg^{2+} with dissolved organic matter (DOM) is represented by complexation with four reactants symbolizing different functional groups such as humic and fulvic acids (Ya, Yb and Yc) and thiols (Ys). Thiol groups contribute to ~0.9 % of the total DOM exchange sites (Skyllberg 2008), in line with the reported sulphur percentage range in DOM (0.5 to 2.0 % in weight; Ravichandran 2004). For humic and fulvic acids, the relative abundance of Ya, Yb and Yc functional groups is 88.1, 11.3 and 0.6 %, respectively. Mass action constants for Hg^{2+} complexation with DOM are taken from Bessinger and Marks (2010) for fulvic and humic acids and from Skyllberg (2008) for thiols (Table 1, left column)

Colloidal transport of Hg (Sen and Khilar 2006; Zhu et al. 2012) is implicitly present in the model by the transport of DOM-bound Hg. Numerical solutions for simulating colloid formation and migration in a more realistic manner exist (Šimůnek et al. 2006) but generally demand numerous specific parameters that are not available for the present case.

Hg sorption to solid organic matter

An approach based on multiple proton/ion exchangers is used to describe the interactions between Hg and immobile SOM. Again, four reactive surface sites are considered (Table 1, right column), denoted as Xa, Xb, Xc (representing oxygen sites of fulvic and humic acids) and Xs (representing thiols). Similarly to DOM, thiol exchange sites represent ~0.9 % of the total SOM, and the relative abundance of Xa, Xb and Xc is the same as that for Ya, Yb and Yc (see "Aqueous speciation and complexation"). For fulvic and humic acids, sorption of H^+, Ca^{2+}, Mg^{2+}, K^+, Na^+, Hg^{2+} and $HgOH^+$ to exchange sites is included in the model. Reactions and exchange constants other than those included in the Thermoddem database are provided in Online Resource 2. For thiol groups, ion exchange is simulated with H^+, Ca^{2+}, Mg^{2+}, K^+, Na^+ and Hg^{2+}. The mass action constants are taken from Bessinger and Marks (2010) for fulvic and humic acids and from Skyllberg (2008) for thiols (Table 1, right column). Exchange reactions are written according to the Gaines-Thomas convention. In soils with Hg background concentrations, thiols are always in excess compared to Hg (Skyllberg 2010). However, in soil systems contaminated by human activities, this may not always be the case.

Dissolution of solid and residual non-aqueous-phase liquid mercury

The dominant solid form of Hg^{2+} in contaminated soil is cinnabar (HgS(s)), which is taken in the current model as the only Hg solid phase. For the simulation of cinnabar dissolution, a rate law is implemented assuming a surface area of 0.23 m^2 g^{-1} (Waples et al. 2005). Since the presence of DOM

Table 1 Equilibrium constants for Hg-DOM complexes (represented by Ya, Yb, Yc and Ys; left column) and for sorption of Hg to SOM (ion exchange assemblage represented by Xa, Xb, Xc and Xs; right column)

Complexation Hg-DOM	Log *k*	Sorption Hg-SOM	Log *k*
$HYa+0.5Hg^{2+}=Hg_{0.5}Ya+H^{+}$	−1.1[a]	$Hg^{2+}+2Xa^{-}=HgXa_2$	3.5[a]
$HYb+0.5Hg^{2+}=Hg_{0.5}Yb+H^{+}$	−7.6[a]	$Hg^{2+}+2Xb^{-}=HgXb_2$	4.3[a]
$HYc+0.5Hg^{2+}=Hg_{0.5}Yc+H^{+}$	−1.8[a]	$Hg^{2+}+2Xc^{-}=HgXc_2$	5.08[a]
$HYa+HgOH^{+}=HgOHYa+H^{+}$	−3[a]	$HgOH^{+}+Xa^{-}=HgOHXa$	7.7[a]
$HYb+HgOH^{+}=HgOHYb+H^{+}$	1.8[a]	$HgOH^{+}+Xb^{-}=HgOHXb$	7.7[a]
$HYc+HgOH^{+}=HgOHYc+H^{+}$	2.0[a]	$HgOH^{+}+Xc^{-}=HgOHXc$	10.2[a]
$2HYs+Hg^{2+}=HgYs_2+2H^{+}$	22.0[b]	$Hg^{2+}+2HXs=HgXs_2+2H^{+}$	15.4[b]

[a] Bessinger and Marks (2010)
[b] Skyllberg (2008)

enhances the solubility and dissolution of cinnabar (Ravichandran 2004), the rate is dependent on DOM concentration in soil water:

$$C(t) = C_0 \exp(-\lambda_{\text{cinn}}\ \text{DOM}\ t) \tag{8}$$

where $C(t)$ is cinnabar concentration at time t [M L^{-3}], C_0 the initial cinnabar concentration in soil [M L^{-3}], DOM the dissolved organic matter concentration at time t [M L^{-3}] and λ_{cinn} the dissolution rate per unit DOM [T^{-1} M^{-1} L^3]. In the numerical simulations presented below, a value of 7.33×10^{-3} day^{-1} $g_{OC}{}^{-1}$ is used for λ_{cinn}, corresponding to the average of the minimum and maximum rates determined by Waples et al. (2005) among 12 different DOM isolates. Since these rates were obtained by batch experiments, they can be regarded as upper limits of the dissolution rate that would take place in unsaturated conditions.

Concerning NAPL dissolution, several approaches exist for characterizing the relationship between mass flux reduction and mass removal. These approaches are usually based on source-depletion models or mass-removal functions (e.g. Jawitz et al. 2005; Brusseau et al. 2008; Basu et al. 2008). However, these models often require additional parameters such as a mass transfer coefficient between the NAPL and the soil solution and the specific interfacial area between phases, which are currently not available for a liquid Hg^0-air-water system. Therefore, a simple dissolution model with a first-order rate equation (after Zhu and Sykes 2004) is implemented:

$$C(t) = C_0 \exp(-\lambda_{\text{NAPL}} t) \tag{9}$$

where $C(t)$ is Hg NAPL concentration at time t [M L^{-3}], C_0 the initial Hg NAPL concentration in soil [M L^{-3}] and λ_{NAPL} the NAPL dissolution rate [T^{-1}]. Due to the paucity of data on Hg NAPL, no dissolution rate could be derived from the literature. Realistic dissolution rates can be approximated to some extent by observed persistence time of Hg NAPL in soils (e.g. Bloom et al. 2003), but this remains a parameter with a high level of uncertainty. An arbitrary rate is fixed such that residual NAPL has a half-life of approximately 2.2 years (Table 2).

Hg reduction and volatilization

Starting from Hg^{2+}, mercury transfer to the atmosphere requires three steps: (i) reduction of Hg^{2+} to Hg^0, (ii) diffusion or mass transport of Hg^0 to the soil surface (in gaseous and aqueous phases) and (iii) diffusion or mass transport of Hg^0 across the soil-air boundary layer into the atmosphere (Schlüter 2000). Soil temperature and Hg adsorption are considered the most important factors driving Hg volatilization (Gabriel and Williamson 2004). Mercury volatilization (or evaporation) has been found to increase with increasing soil temperature (review by Schlüter 2000), and direct sunlight can enhance the reduction of Hg^{2+} to Hg^0 (Gabriel and Williamson 2004). The presence of Hg sorption sites decreases Hg volatilization as Hg^{2+} sorbed to a soil component has a lower tendency to be reduced compared to free Hg^{2+} in solution (Schlüter 2000). For soils contaminated with non-volatile mercury species, it can be expected that the production of volatile mercury (instead of meteorological conditions) is the evaporation rate-limiting process (Schlüter 2000).

The transformation of aqueous Hg^{2+} into gaseous Hg^0 involves two reactions, namely a reduction reaction (Eq. 10) and a volatilization reaction (Eq. 11):

$$Hg^{2+} + H_2O \leftrightarrows Hg^0(aq) + \tfrac{1}{2} O_2 + 2H^{+} \quad \log k = -20.649 \tag{10}$$

$$Hg^0(aq) \leftrightarrows Hg^0(g) \quad \log k = 0.924 \tag{11}$$

where the log k values were recovered from the Thermoddem database. Thermodynamically, Hg volatilization seems not favoured in the present case under the (assumed) prevailing oxidizing conditions. However, Hg(g) emissions are often observed at contaminated sites. Therefore, the reduction of Hg^{2+} to Hg^0 is described by a first-order kinetic reaction:

$$C(t) = C_0 \exp(-\lambda_{\text{red}} t) \tag{12}$$

where $C(t)$ is the concentration of Hg^{2+} in solution at time t [M L^{-3}], $C_0(t)$ the initial concentration of Hg^{2+} [M L^{-3}] and

λ_{red} the Hg^{2+} reduction rate [T^{-1}]. This reaction is applied to the top 5 cm of the soil profile, reflecting the influence of sunlight and temperature to the topsoil only. The parameter values used for processes related to the reduction and volatilization of Hg are given in Table 2. In the present study, the value of λ_{red} (6.91×10^{-6} day^{-1}) is taken from Scholtz et al. (2003), who selected it to match measured Hg volatilization (between 1.2×10^{-2} and 4.5×10^{-2} $\mu g\ m^{-2}\ h^{-1}$, data from Carpi and Lindberg 1998 at soils with a background Hg concentration). For contaminated sites, the fitted reduction rate might be higher, as suggested for instance by $Hg^0(g)$ emission rates of 0.01 to 0.85 $\mu g\ m^{-2}\ h^{-1}$ measured by Rinklebe et al. (2010).

DOM sorption to minerals

DOM sorption to mineral surfaces is modelled using a Langmuir isotherm. The PHREEQC model for surface complexation is used, as follows:

$$DOM_{Sor} = \frac{K_L\, S_{max}\, DOM_f}{1 + K_L\, DOM_f} - b \qquad (13)$$

where DOM_{Sor} is the amount of DOM sorbed [mg kg^{-1}], K_L the coefficient of binding affinity [−], S_{max} the maximum adsorption capacity [mg kg^{-1}], DOM_f the final equilibrium concentration [mg kg^{-1}] and b a desorption term [mg kg^{-1}]. K_L and S_{max} values (Table 2) were taken from the Langmuir isotherm (with final concentration in the formulation) fitted by Kothawala et al. (2008). Among their 52 mineral soil samples grouped into nine different soil horizons, parameters for DOM sorption in an Ah horizon (seven samples) were selected. This corresponds to the top horizon of our hypothetical soil profile (see "Hypotheses for the test case"), where most of the Hg transformation and (de)sorption processes will take place. The desorption term b (a correction for "native" adsorbed DOM on minerals) is set to 0. The desorption term is generally useful to fit sorption batch experiments, but since we are dealing with a numerical simulation of a hypothetical soil profile, we have no reason to consider native adsorbed DOM and simply let the incoming DOM progressively fill the adsorption sites.

Mathematical and numerical implementation

Simulators have been recently developed for simulating reactive transport in the subsurface, among which are MIN3P (Mayer et al. 2002), PHT3D (Prommer et al. 2003), HYDROGEOCHEM (Yeh et al. 2004), PHWAT (Mao et al. 2006), HP1, CRUNCHFLOW (Steefel 2009), PHAST (Parkhurst et al. 2010), RICH-PHREEQ (Wissmeier and Barry 2010). From these, MIN3P, HYDROGEOCHEM, HP1, CRUNCHFLOW and RICH-PHREEQ can simulate variably saturated flow. The code HP1 was chosen to implement the conceptual model presented above. HP1 (available at http://www.pc-progress.com) is based on the coupling of HYDRUS-1D (Šimůnek et al. 2008) for water and solute transport and PHREEQC (Parkhurst and Appelo 1999) for geochemical calculations. It has strong capacities to solve reactive transport problems in unsaturated soils by allowing selection of different relevant boundary conditions. The program calculates, for example, actual evapotranspiration by including moisture-dependent water uptake by plant roots. Because of the flexible way of setting up complex reaction networks in PHREEQC, a property inherited by HP1, the different geochemical reactions involving Hg can be implemented in a straightforward way. This also allows incorporating additional processes such as uptake by roots, colloidal transport or other rate laws in future studies.

Hypotheses for the test case

A test case is developed for the numerical simulation of Hg fate and transport in a variably saturated soil system. Three possible sources of Hg contamination are considered: mercury

Table 2 Parameterization of the hypothetical test case

Parameter	Value	Unit	Reference
Initial Hg concentration	135	mg kg^{-1}	–
Cinnabar dissolution rate	7.33×10^{-3}	$day^{-1}\ g_{OC}{}^{-1}$	Waples et al. (2005)
NAPL dissolution rate	8.64×10^{-4}	day^{-1}	–
Hg^{2+} reduction rate	6.91×10^{-6}	day^{-1}	Scholtz et al. (2003)
$Hg^0(g)$ diffusion coefficient in air	0.119	$cm^2\ s^{-1}$	Massman (1999)
Atmospheric background Hg(g) concentration	1	ng m^{-3}	–
DOM (in rainwater boundary solution)	50	mg L^{-1}	Don and Schulze (2008)
Exchange site density of HA and FA (SOM top 30 cm)	5.3	meq $g_{OC}{}^{-1}$	Gustafsson (1999)
Exchange site density of thiols (SOM top 30 cm)	0.047	meq $g_{OC}{}^{-1}$	Skyllberg (2008)
K_L sorption DOM to soil minerals	5.6×10^{-3}	–	Kothawala et al. (2008)
S_{max} max. adsorption capacity of DOM to minerals	355	mg kg^{-1}	Kothawala et al. (2008)

release from (i) cinnabar (HgS(s)) dissolution, (ii) Hg NAPL degradation and (iii) mercuric chloride ($HgCl_2$(aq)) directly added to the soil pore water. These three sources are among the most frequent Hg species and phases found in mercury-contaminated land.

The model is applied on a hypothetical 1-m-deep soil profile with a homogeneous sand texture. The van Genuchten-Mualem model is used as input for solving the Richards equation for water flow, using the following hydraulic parameters: θ_s=0.43 cm^3 cm^{-3}, θ_r=0.045 cm^3 cm^{-3}, α=0.145 cm^{-1}, n=2.68 and K_{sat}=712.8 cm day^{-1}.

A 50-year time series of daily atmospheric boundary conditions is used, consisting of 25 years of data from observed precipitation and calculated potential evapotranspiration from Dessel (Campine region, north-eastern Belgium), repeated once. This approach allows simulating spatial and temporal variation in water content, air content and water fluxes which may affect the transport of contaminants in the vadose zone (Jacques et al. 2008a). Average precipitation and potential evapotranspiration are ~820 and ~510 mm $year^{-1}$, respectively. A grass cover is assumed at the soil surface with a uniform rooting depth of 30 cm (no Hg uptake by the roots). Potential evapotranspiration is split into soil evaporation and transpiration based on the leaf area index. The average actual evapotranspiration simulated is about 260 mm $year^{-1}$, with 100 mm $year^{-1}$ of evaporation and 160 mm $year^{-1}$ of transpiration. The average water flux at the bottom of the 1-m profile is about 560 mm $year^{-1}$. The hydraulic boundary condition at the bottom of the soil profile is free drainage (deep ground water) and oxidizing conditions are assumed.

Initial soil solution and rainwater composition are taken from the Dutch "National Precipitation Chemistry Network" (Stolk and 2001 Landelijk Meetnet Regenwatersamenstelling - Meetresultaten, 1999), which can be considered as representative of the conditions in the Campine region. The source of DOM in the soil system is considered to be infiltrating rainwater, i.e. a constant DOM concentration is included in the initial and boundary solution composition. A value of 50 mg L^{-1} is chosen, corresponding to the median of the range of concentrations (30 and 70 mg L^{-1} in spring and autumn, respectively) measured by Don and Schulze (2008) on a site (Kaltenborn) with a soil texture similar to that of the test case.

A more realistic approach is by explicitly modelling the soil carbon cycle with the production of DOM from fresh and humified organic matter. However, this mechanistic model falls outside the scope of the present approach because of model uncertainty in the soil carbon cycle, as well as parameter uncertainty.

Estimation of the exchange capacity assumed a soil bulk density of 1.5 g cm^{-3}, a uniform SOM content of 1 % in the top 30 cm of the soil profile and an exchange site density of 5.3 meq g_{OC}^{-1} (humic and fulvic acids; Gustafsson 1999) and 0.047 meq g_{OC}^{-1} (thiol sites; Skyllberg 2008) (Table 2). Hg is thus only retained by the solid phase in the top 30 cm; below this zone, it is assumed that the organic matter content is very low. DOM sorption to minerals occurs over the entire profile.

The composition of SOM can vary strongly between different vegetation covers, soil types and climate conditions. The exchange site density of thiols used here is considered typical of a wetland sediment (Skyllberg 2008) and acceptable for the present hypothetical case. For a real-case application, site-specific values of SOM composition may be preferable to determine the relative abundance of Hg and strong binding sites, as this is a sensitive input variable (Leterme et al. 2013).

The first three simulations presented hereafter use a different Hg source in the topsoil: cinnabar for simulation A, Hg NAPL (simulation B) and aqueous mercuric chloride (simulation C). Contrary to what is modelled for cinnabar and NAPL where a dissolution release mechanism is assumed, mercuric chloride as a source of contamination is added to the soil solution in one single event. Initial Hg contamination is assumed to be uniformly spread in the top 10 cm of the soil profile, with a concentration of 135 mg [Hg]kg^{-1} [soil] (realistic for a site of anthropogenic contamination; see, for example, Bloom et al. 2003; Boszke et al. 2008; Bollen et al. 2008).

Four simulations (D to G) are performed with the same initial Hg concentration but using combinations of the three different Hg sources: 50 % HgS(s) and 50 % Hg NAPL, 50 % Hg NAPL and 50 % $HgCl_2$(aq), 50 % HgS(s) and 50 % $HgCl_2$(aq), and a case with one third of each.

The model outputs considered are (i) Hg volatilized to the atmosphere, (ii) Hg leached from the 1-m-deep soil profile, (iii) Hg still present in the originally contaminated soil horizon (top 10 cm) and (iv) Hg present in the biologically active soil zone below the originally contaminated soil horizon (between 10 and 30 cm). Results are expressed in percentages of initial Hg contamination.

Results and discussion

Hg^{2+} speciation related to SOM and DOM

Figure 2 shows the Hg sorption isotherm with the total Hg concentration ranging from 0.05 to 1 mmol L^{-1}. At low Hg concentrations, sorption occurs exclusively on thiol groups, due to their higher sorption strength (Table 1). This is in accordance with Skyllberg (2010), who suggested that under oxic conditions with 1 % SOM and low or moderate Hg contamination (≤0.1 mg [Hg]kg^{-1} [soil]), the concentration of Hg may be exclusively bound to thiol groups. Sorption on HA and FA starts at a total Hg concentration between 0.3 and 0.4 mmol L^{-1} (first via HgOHXa and HgOHXc) when thiol sorption sites become saturated, and peaks at a total Hg

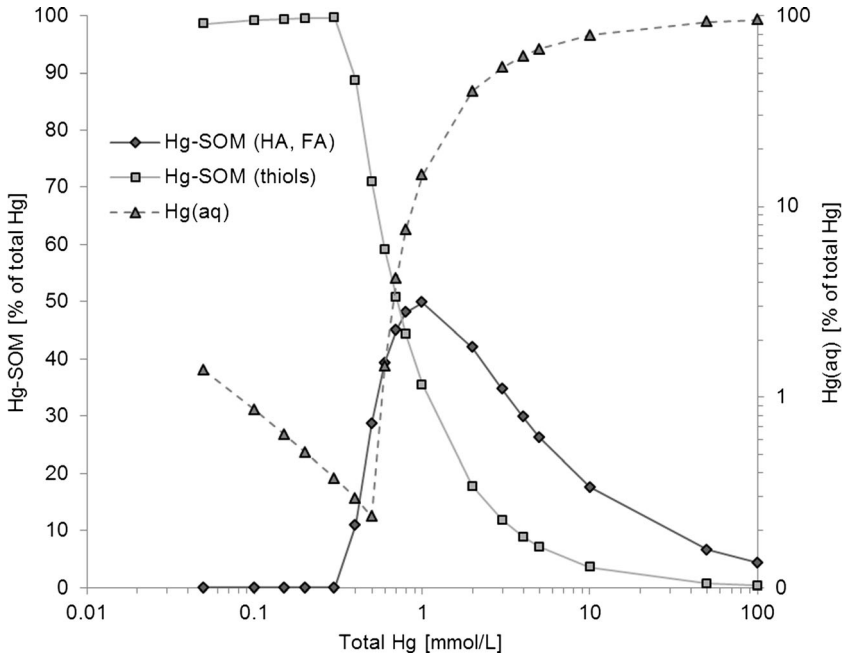

Fig. 2 Sorption isotherm of Hg on SOM (*plain lines*) and Hg in aqueous phase (*dotted line with triangles*). Sorption to thiol groups (Xs in Table 1) and humic and fulvic acids (Xa, Xb, Xc in Table 1) are distinguished (*light grey line with squares* and *dark grey line with diamonds*, respectively)

concentration of 1 mmol L^{-1}. The presence of ~1 % of aqueous Hg at low total Hg concentrations is due to the complexation of Hg^{2+} with strongly binding DOM thiol groups. The minimum concentration of aqueous Hg is found at 0.5 mmol L^{-1} of total Hg. At higher total Hg concentrations, the increase of Hg cannot be fully assimilated by HA and FA sorption sites (due to competition of other cations) and $Hg(OH)_2(aq)$ starts to form.

Figure 3 shows how the apparent distribution ratio (K_d expressed as the concentration of Hg-SOM [mol L^{-1}] over the total aqueous concentration Hg(aq) [mol L^{-1}]) changes with increasing total Hg concentration, in the presence (50 mg L^{-1}) or absence of DOM in the aqueous phase. At

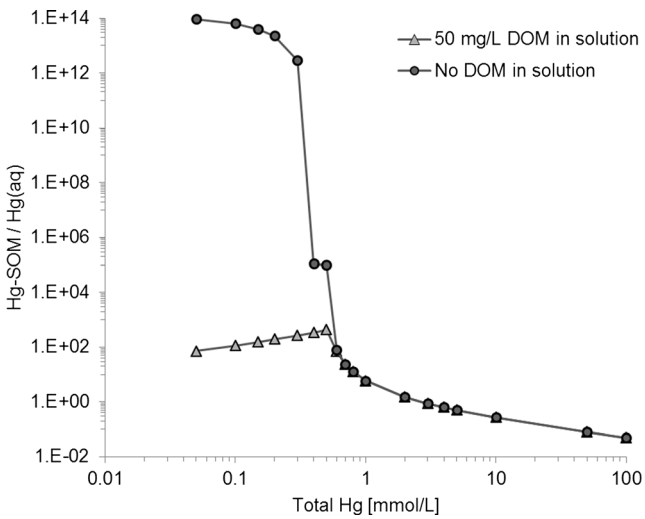

Fig. 3 Mercury apparent K_d with 50 mg L^{-1} DOM (*triangles*) or no DOM (*circles*) in the soil solution

Hg total concentrations lower than ~0.5 mmol L^{-1}, the presence of DOM in the solution has a high impact on the apparent K_d (more than 10 orders of magnitude smaller than in the absence of DOM). It follows from Table 1 that DOM thiols are responsible for this lower apparent K_d, as only the thiols involving complexation reaction have higher equilibrium constants than the Hg sorption reactions. Above 0.5 mmol L^{-1} of total Hg, sorption sites are saturated and the presence of DOM has no impact on the apparent K_d.

Simulation A: cinnabar (HgS(s))

The values of the cinnabar dissolution rate (λ_{cinn}, Table 2) and DOM concentration in rain resulted in 50 % of the cinnabar remaining in its initial form even after 50 years (Table 3). Figure 4a shows the profile of cinnabar concentration after 5, 10, 25 and 50 years. The slightly faster dissolution at the surface is due to the influence of DOM on the dissolution rate (Eq. 8); deeper in the soil profile, more DOM is sorbed to minerals. Alternatively, DOM concentration near the surface can be quite high during dry soil conditions due to evaporation and some upward transport which is to a given extent similar to the effect of Cl accumulation on Cd fate as mentioned by Jacques et al. (2008b). Figure 4b shows the profile of Hg sorbed to SOM. After 50 years, about 10 % of the initial contamination is present in the top 10-cm in the form of Hg^{2+} sorbed to SOM (Table 3).

The most favourable reaction from a thermodynamic viewpoint is the complexation of Hg^{2+} with DOM thiols (Table 1). However, these functional groups are the less abundant among the four postulated DOM functional groups. Therefore, if the initial release of free Hg^{2+} ions in the soil solution is slow

Table 3 Results of simulations A to C after 5, 25 and 50 years, expressed in percentage of the initial Hg contamination

	Hg volatilized (%)	Hg leached (%)	Hg in top 10 cm (%)	Hg-SOM between 11 and 30 cm (%)
A, 100 % cinnabar (HgS(s))				
After 5 years	<0.1	0.2	HgS(s), 93.6 Hg-SOM, 4.2	2.0
After 25 years	<0.1	6.6	HgS(s), 70.7 Hg-SOM, 11.7	11.0
After 50 years	<0.1	19.1	HgS(s), 50.0 Hg-SOM, 10.1	20.7
B, 100 % Hg NAPL				
After 5 years	<0.1	0.3	Hg NAPL, 20.6 Hg-SOM, 74.4	4.7
After 25 years	0.2	7.3	Hg-SOM, 72.3	20.4
After 50 years	0.2	20.5	Hg-SOM, 44.9	34.5
C, 100 % $HgCl_2$(aq)				
After 5 years	<0.1	1.6	Hg-SOM, 42.0	56.4
After 25 years	<0.1	13.7	Hg-SOM, 23.8	62.4
After 50 years	<0.1	32.1	Hg-SOM, 1.8	66.0

enough, a higher proportion of the released Hg will be transported via these highly stable Hg complexes (as shown by the higher percentage of Hg in solution at low Hg concentrations; Fig. 2) and less retardation occurs than in the case of a high release rate. Figure 5 shows Hg^{2+} leaching concentrations at the bottom of the soil profile over time. After 15 to 20 years, Hg^{2+} concentrations stabilize between 10^{-4} and 10^{-3} μg L^{-1}. Simulated Hg^{2+} concentrations increase in dry periods (due to root water uptake which results in higher DOM concentration in the subsurface pore water), but appear to remain above a certain level (i.e. >10^{-4} μg L^{-1}), which is actually determined by the concentration of thiols in the soil solution.

The effect of the four different exchange sites and corresponding mass action constants that are inversely proportional to their abundance is reflected in the evolution of the Hg leached/Hg sorbed ratio in the 11–30-cm interval. This ratio is equal to 0.1 after 5 years, 0.6 after 25 years and finally ~1 after 50 years (Table 3). In other words, when the thiol groups of SOM are occupied by sorbed Hg relatively early in the simulation, HA and FA sorption sites are still available. Over time, HA and FA sites progressively sorb the additional Hg^{2+} released from cinnabar dissolution, but Hg leaching is proportionally more important as the sorption bonds are less strong compared to thiols (Table 1).

Simulated Hg volatilization was negligible (<0.1 % of the initial contamination). This is mainly due to the fact that the reduction rate depends on the total Hg^{2+} concentration in the aqueous phase, i.e. the free Hg^{2+}, the inorganic and organic aqueous complexes of Hg^{2+}, and not on sorbed species. As

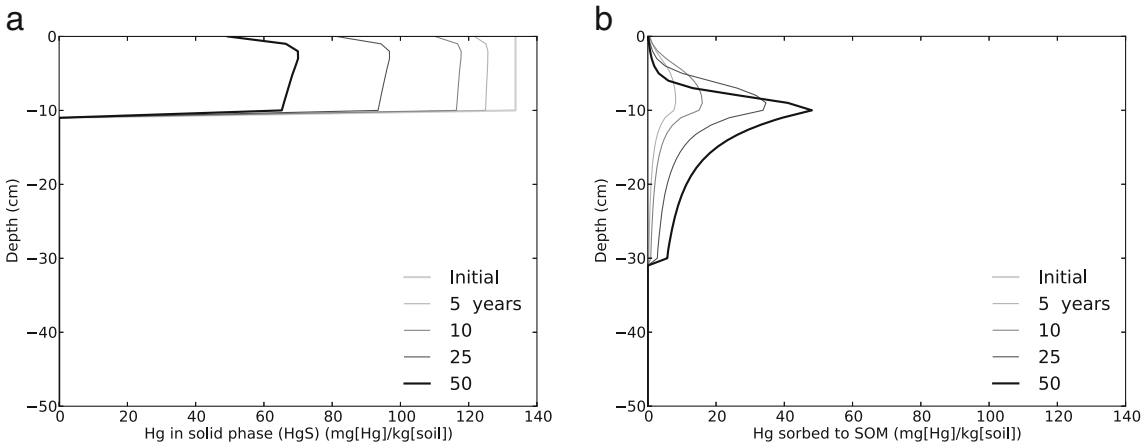

Fig. 4 Depth distribution of Hg (**a**) in solid phase (HgS) and (**b**) sorbed to SOM at t=0, 5, 10, 25 and 50 years for the simulation with cinnabar as the contamination source. Note that, for clarity, the *y-axis* stops at 50 cm depth

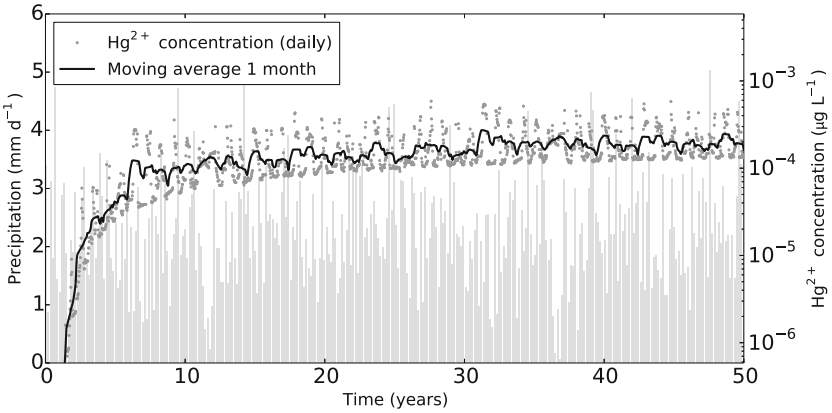

Fig. 5 Hg^{2+} leaching (µg m^{-2} day^{-1}) over time for simulation A with cinnabar (HgS(s)) as the contamination source. *Grey dots* are daily simulated fluxes at the bottom of the soil profile. The *black line* is the result of a moving average (window, 31 days) on the daily data. *Grey bars* show the surface precipitation input (averaged every 2 months for clarity). Note that the *y*-scale is logarithmic for Hg^{2+} leaching

Hg^{2+} concentration in the aqueous phase is relatively low at any time, Hg reduction and volatilization are consequently limited. Simulated Hg^0 flux was never above 10^{-8} µg m^{-2} h^{-1}. For comparison, Rinklebe et al. (2010) measured 0.01 to 0.85 µg m^{-2} h^{-1} Hg emission from heavily polluted floodplain soils.

Simulation B: Hg NAPL

Simulated NAPL dissolution is faster than that of cinnabar, but in the case of NAPL, the dissolution rate is chosen arbitrarily to be dissolved in a period of about 25 years and is not based on any laboratory or field data. Panels a and b of Fig. 6 show the concentration profiles over time for Hg NAPL and Hg sorbed to SOM, respectively. After 25 years, no more Hg is present as NAPL, but almost 75 % of the initial mercury remains sorbed to SOM in the top horizon (Table 3). This sequence of Hg transformation, from the initial Hg^0(l) to Hg^{2+} and then binding to SOM, was observed in studies of different contaminated sites (e.g. Slowey et al. 2005; Boszke et al. 2008). Biester et al. (2002) similarly observed that even after high-contamination events, very few Hg^0 persisted in liquid form: Hg^0 was either rapidly volatilized or more slowly oxidized to Hg^{2+}.

Figure 6b shows that within the time frame of the simulation, maximum Hg concentration is found at the bottom of the initially contaminated horizon. This reflects a concentration profile resulting from a past contamination episode, as opposed to typical concentration profiles of heavy metals decreasing with depth, which indicates continuous enrichment at the surface, for example via irrigation using wastewater (Abdu et al. 2011; Liu et al. 2014).

The faster release of Hg from the source compared to cinnabar produces only a slight increase in leaching (20.5 and 19.1 % after 50 years for the NAPL and cinnabar sources, respectively), but Hg sorption to SOM in the topsoil increases significantly (44.9 % of the initial Hg after 50 years vs. 10.1 % in simulation A). This is due to the (relatively) limited amount of DOM thiols in infiltrating rainwater; i.e. above a certain concentration, the extra Hg released in soil water is less strongly bonded to DOM HA and FA or to inorganic ligands and is thus more prone to sorption.

The maximum concentration of Hg sorbed to SOM (Fig. 6b) reaches almost the initial NAPL concentration

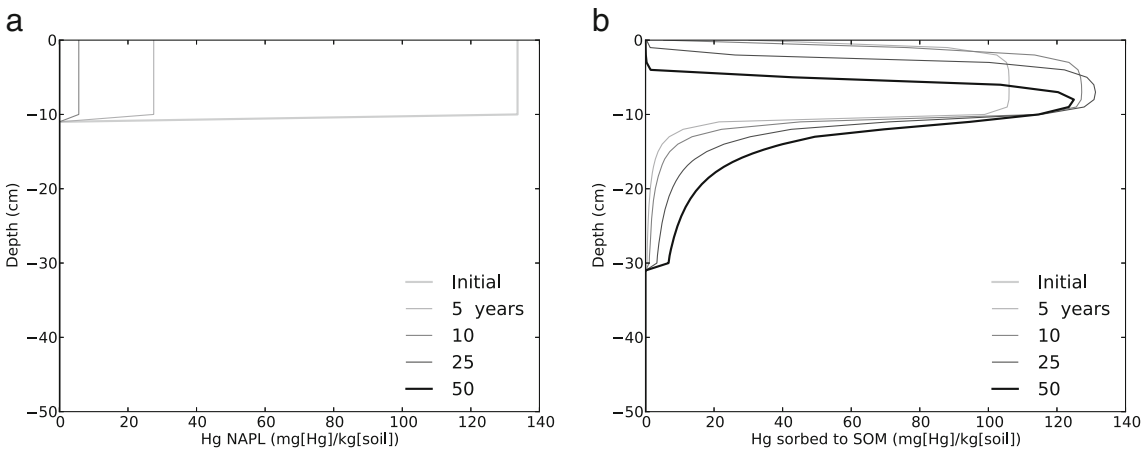

Fig. 6 Depth distribution of Hg **a** in non-aqueous phase liquid (NAPL) and **b** sorbed to SOM at t=0, 5, 10, 25 and 50 years for simulation B with NAPL as the contamination source. Note that, for clarity, the *y-axis* stops at 50 cm depth

(Fig. 6a) and occurs after ~25 years, corresponding to the end of Hg release from the NAPL source.

Simulation C: mercuric chloride ($HgCl_2$(aq))

An increased amount of leaching was simulated when considering mercuric chloride as a contamination source (Table 3), the reason being that all Hg is instantaneously released in the aqueous phase (contrary to simulations A and B in which Hg was progressively released) and, consequently, the maximum sorption capacity for Hg is rapidly reached. Therefore, a significant part of Hg migrates below the original contamination horizon in the early time steps.

Figure 7 shows the percentage of SOM-sorbed Hg relative to the initial contamination expressed as cumulative amount between the soil surface and a given depth (y-axis) as a function of time (x-axis). For example, after the first time step, 42.8 % of the initially aqueous Hg is sorbed to SOM in the top 10 cm and about 19.5 % is sorbed to SOM between 11 and 30 cm depth (thus, 62.3 % is sorbed in the top 30 cm) while the remaining 37.7 % is still in the form of aqueous Hg. The SOM-sorbed mercury rapidly increases up to ~100 %, which is indicated by the dark red zone at a depth of about 25 cm at the beginning of the simulations (smaller than ~5 years). Within this time period, the amount of Hg in the aqueous phase is minimal. The percentage of SOM-sorbed Hg decreases over time as a result of leaching, induced mainly by Hg complexation with DOM thiols. As illustrated in Fig. 3, at low concentrations of total Hg, the apparent K_d is drastically lowered in the presence of DOM. The thiol groups of DOM are the main agents of Hg leaching, and the regular input (via rainwater) of DOM into the soil solution results in the long-term decrease of SOM-sorbed Hg. After 50 years, there is almost no more Hg in the top 10 cm and 32.1 % of the initial contamination has leached (Table 3).

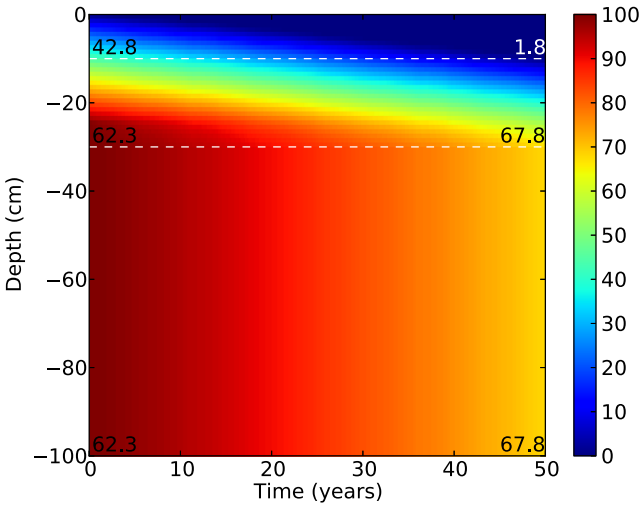

Fig. 7 Cumulative depth distribution over time of Hg sorbed to SOM (in % of total initial Hg) for simulation C with mercuric chloride ($HgCl_2$(aq)) as the contamination source

Simulations D to G: combinations of different Hg sources

Figure 8 shows the results after 5, 25 and 50 years of the simulations combining different Hg contamination sources. As already observed in simulations A and B, cinnabar dissolution is half completed after 50 years, while complete NAPL dissolution occurs within the first 25 years. This has consequences on the amount of Hg available in the aqueous phase for sorption and leaching, especially at the beginning of the simulations. However, because the NAPL dissolution rate is arbitrarily fixed, conclusions that stem from the relative dissolution rates of cinnabar and Hg NAPL have to be taken with caution.

Although Hg leaching starts earlier when $HgCl_2$(aq) is present as a source of contamination, the percentage of leaching after 50 years remains between 20 and 22 % for all four simulations D to G. This suggests that, on the long term, leaching does not depend much on the type of contamination and the release mechanisms (instantaneous compared to dissolutional release) but rather on factors related to the concentration of complexing agents and sorption capacity. A global sensitivity analysis performed on the main parameters and processes of the model (but not combining different Hg sources) showed that for leaching after 50 years, the most sensitive factors are Hg sorption strength to HA and FA, DOM concentration and initial Hg concentration (Leterme et al. 2013). The sorption strength to HA and FA (less strongly binding but much more abundant than thiol groups) largely determines how much of the initial mercury can be retained in the polluted soil horizon. If the sorption capacity on a contaminated site is estimated insufficient for preventing significant leaching, one can immobilize mercury by increasing the number of sorption sites with a high binding strength (e.g. using powdered activated carbon as in Bessinger and Marks 2010).

The presence of $HgCl_2$(aq) as one of the sources of Hg contamination (simulations E to G) results in a higher percentage of mercury sorbed to SOM in the 11–30-cm interval, below the originally contaminated horizon. This is because the instantaneously released mercury results in higher Hg concentrations in the aqueous phase. Consequently, due to the limited amount of DOM thiol ligands, a relatively lower percentage (compared to the slower release of Hg from cinnabar or NAPL dissolution) of the initial mercury is transported via strongly bound Hg-DOM complexes and, therefore, sorption can take place at a deeper level in the soil profile.

Globally, the results presented in Fig. 8 provide intermediate values of the output indicators compared to simulations A to C dealing with individual contamination sources.

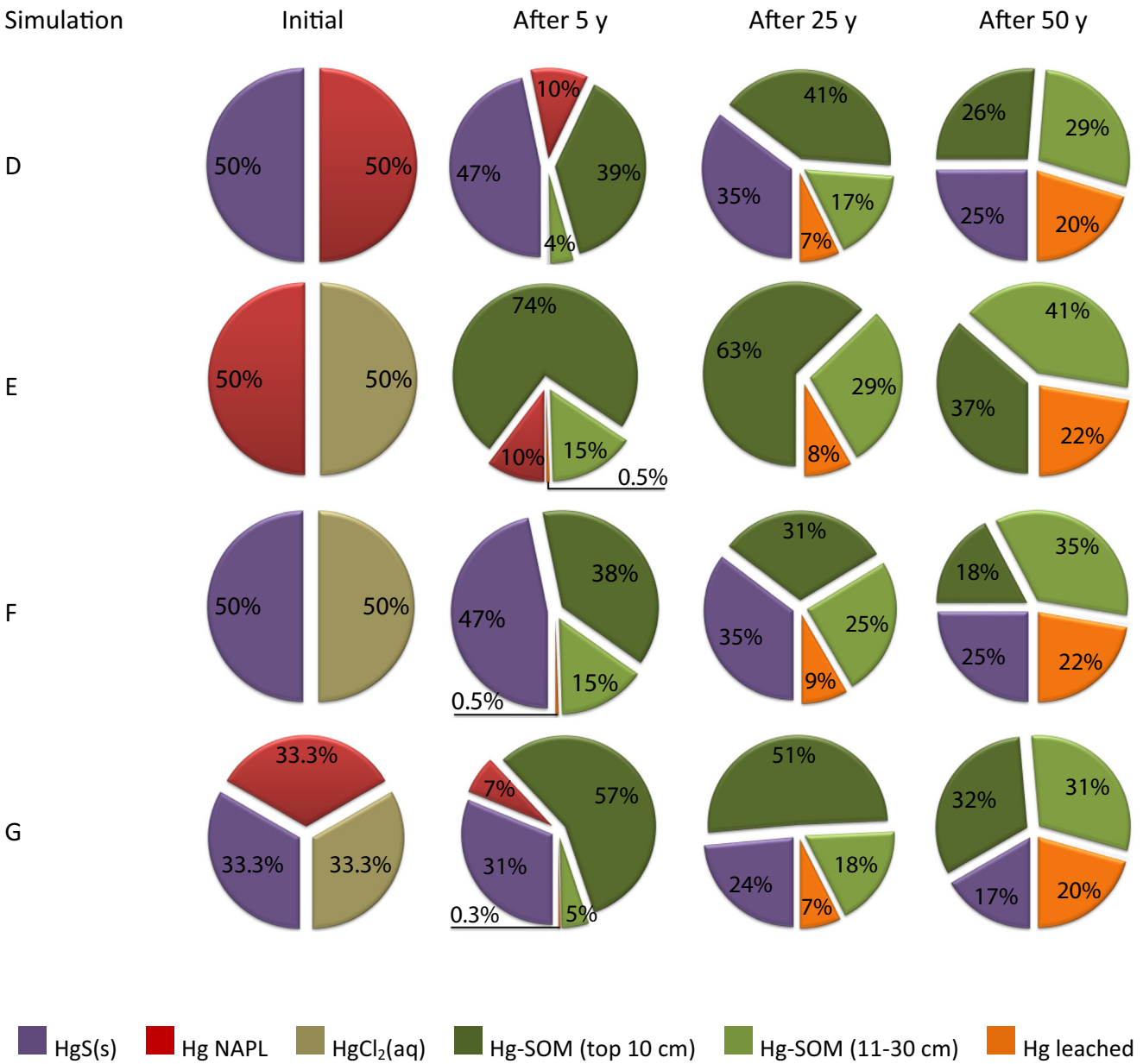

Fig. 8 Pie charts showing the evolution over time (initial and after 5, 25, 50 years) of different Hg species/phases and leaching for simulations D to G (combinations of different Hg contamination sources)

Potential applications to risk management and remediation studies

Coupling unsaturated flow conditions with a detailed chemical modelling of Hg fate gives interesting perspectives regarding the management of contaminated sites. First and foremost, this type of numerical model allows investigating likely transport pathways on the (very) long term. This may prove very useful to anticipate future exposure pathways that could be unexpected in the first place. The slow kinetics of some of the Hg speciation and transformation processes (such as cinnabar dissolution) may delay the occurrence of leaching or volatilization. Under certain conditions (high number of sorption sites), this delay may typically be of the order of several decades, i.e. potentially beyond site monitoring or management time frames (Leterme et al. 2013). If such exposure pathways are not detected by real-time site monitoring, numerical modelling such as presented here has the potential to help assess future human or ecological exposure.

Furthermore, using the present model in a sensitivity analysis allows identifying sensitive parameters for which site-specific information should be collected (Leterme et al. 2013). In this way, a better understanding of the dynamics of site pollution and possible dispersion pathways may be obtained.

Another useful application is the simulation of potential remediation strategies for contaminated sites, such as demonstrated by Bessinger and Marks (2010). If the site is well characterized, site-specific model parameterization is possible and allows simulating and comparing of different remediation options (e.g. removal of the most contaminated soil layer, addition of powdered activated carbon, impervious cover…). This information may bring additional confidence to a cost-benefit analysis for designing remediation plans.

Conclusions

A one-dimensional model was developed for mercury fate and transport in soils. The processes considered relevant under the assumptions of anthropogenic contamination and oxic conditions were Hg transport and speciation in gaseous and aqueous phases (with transport of Hg-DOM complexes as a surrogate for colloid transport), Hg sorption to SOM, cinnabar and Hg NAPL dissolution, Hg^{2+} reduction and volatilization, and DOM sorption to minerals. This model was numerically implemented in the coupled reactive transport simulator HP1 for variably saturated flow conditions.

First, Hg sorption isotherm and apparent K_d were presented, based on the thermodynamic database and organic matter composition used in the model. At low Hg concentrations (<0.5 mmol L^{-1}), the apparent K_d was found to be highly sensitive to the presence of DOM in solution. Hg^{2+} complexation with DOM thiols resulted in a decrease of the apparent K_d value by more than 10 orders of magnitude (compared to K_d in the absence of DOM).

A hypothetical test case was then presented, simulating 50 years of daily atmospheric input. The effect was studied on a sandy soil profile, with three different phases of mercury contamination: solid (cinnabar), liquid Hg, aqueous mercuric chloride and combinations of these different sources. Depending on the source, Hg leaching after 50 years varied between 19 and 32 % of the initial amount of Hg. Hg volatilization was negligible in all simulations because the Hg^{2+} reduction rate was a function of the aqueous concentration of Hg^{2+}, which was always found to be very low.

The thiol groups in DOM were identified as the main complexing agent responsible for Hg leaching. Hg complexation with inorganic ligands was in general not important, except in the case of a massive and instantaneous release of aqueous Hg. In our simulations, Hg^{2+} concentrations in the aqueous phase outnumbered the amount of DOM thiols only when the instantaneous release of $HgCl_2$(aq) was one of the sources (simulations C, E, F and G). This eventually produces a migration of inorganic Hg species below the contaminated horizon and sorption deeper in the soil profile.

Thiol groups are also the most favoured sorption sites in SOM. However, since the present model was developed for contaminations from anthropogenic activities, high Hg concentrations were simulated and the (in SOM) more abundant oxygen groups (humic and fulvic acids) were also important in determining the fate and mobility of Hg in the soil. After a simulated period of time of 50 years, the amount of Hg sorbed on SOM in or below the contaminated horizon is ranging from 30.8 to 79.4 %. This variability is largely due to the presence or absence of cinnabar as a contamination source (which, in our test case, is only half dissolved after 50 years). Potential applications of the model to the management of contaminated sites were shortly discussed, including the assessment of likely transport and exposure pathways and the simulation of possible remediation actions.

A global sensitivity analysis of the model has been done (Leterme et al. 2013). However, at this point, no model calibration has been performed. Therefore, a next step is to test our model against data from a real case study of Hg contamination in the unsaturated zone. By using detailed speciation data of Hg contamination in soils and confronting numerical simulations to field observations, the model could help to gain insights in the fate and transport of mercury and thus improve our ability to mitigate the exposure to this contaminant.

Acknowledgments The present study is part of the IMaHg project (Enhanced knowledge in mercury fate and transport for Improved Management of Hg soil contamination), which aims at providing recommendations to improve management of sites contaminated by mercury within the SNOWMAN funding framework. This particular work was done with the financial support of the Public Waste Agency of Flanders (OVAM). Prof. T. Leyssens is acknowledged for his help in improving the manuscript.

References

Abdu N, Abdulkadir A, Agbenin JO, Buerkert A (2011) Vertical distribution of heavy metals in wastewater-irrigated vegetable garden soils of three West African cities. Nutr Cycl Agroecosyst 89(3): 387–397

Andrews JC (2006) Mercury speciation in the environment using x-ray absorption spectroscopy. In: Atwood D (ed) Recent developments in mercury science, vol 120. Structure and bonding. Springer Berlin, Heidelberg, pp 1–35. doi:10.1007/430_011

Baes CF, Mesmer RE (1976) The hydrolysis of cations. Wiley, New York

Basu NB, Fure AD, Jawitz JW (2008) Simplified contaminant source depletion models as analogs of multiphase simulators. J Contam Hydrol 97(3–4):87–99

Bernaus A, Gaona X, van Ree D, Valiente M (2006) Determination of mercury in polluted soils surrounding a chlor-alkali plant: direct speciation by X-ray absorption spectroscopy techniques and preliminary geochemical characterisation of the area. Anal Chim Acta 565(1):73–80

Bessinger B, Apps JA (2005) The hydrothermal chemistry of gold, arsenic, antimony, mercury and silver. Report LBNL-57395, Lawrence Berkeley National Laboratory, USA

Bessinger BA, Marks CD (2010) Treatment of mercury-contaminated soils with activated carbon: a laboratory, field, and modeling study. Remediat J 21(1):115–135. doi:10.1002/rem.20275

Bessinger BA, Vlassopoulos D, Serrano S, O'Day PA (2012) Reactive transport modeling of subaqueous sediment caps and implications for the long-term fate of arsenic, mercury, and methylmercury. Aquat Geochem 18(4):297–326. doi:10.1007/s10498-012-9165-4

Biester H, Gosar M, Müller G (1999) Mercury speciation in tailings of the Idrija mercury mine. J Geochem Explor 65(3):195–204

Biester H, Müller G, Schöler HF (2002) Binding and mobility of mercury in soils contaminated by emissions from chlor-alkali plants. Sci Total Environ 284(1–3):191–203

Blanc P, Lassin A, Piantone P, Azaroual M, Jacquemet N, Fabbri A, Gaucher EC (2012) Thermoddem: a geochemical database focused on low temperature water/rock interactions and waste materials. Appl Geochem 27(10):2107–2116. doi:10.1016/j.apgeochem.2012.06.002

Bloom NS, Preus E, Katon J, Hiltner M (2003) Selective extractions to assess the biogeochemically relevant fractionation of inorganic mercury in sediments and soils. Anal Chim Acta 479(2):233–248

Bollen A, Wenke A, Biester H (2008) Mercury speciation analyses in HgCl2-contaminated soils and groundwater-implications for risk assessment and remediation strategies. Water Res 42(1–2):91–100

Boszke L, Kowalski A, Astel A, Barański A, Gworek B, Siepak J (2008) Mercury mobility and bioavailability in soil from contaminated area. Environ Geol 55(5):1075–1087. doi:10.1007/s00254-007-1056-4

Brusseau ML, DiFilippo EL, Marble JC, Oostrom M (2008) Mass-removal and mass-flux-reduction behavior for idealized source zones with hydraulically poorly-accessible immiscible liquid. Chemosphere 71(8):1511–1521

Carpi A, Lindberg SE (1998) Application of a teflon dynamic flux chamber for quantifying soil mercury flux: tests and results over background soil. Atmos Environ 32(5):873–882

Cox JD, Wagman DD, Medvedev VA (1989) CODATA key values for thermodynamics. Hemisphere Pub. Corp.

Davis A, Bloom NS, Que Hee SS (1997) The environmental geochemistry and bioaccessibility of mercury in soils and sediments: a review. Risk Anal 17(5):557–569. doi:10.1111/j.1539-6924.1997.tb00897.x

Don A, Schulze E-D (2008) Controls on fluxes and export of dissolved organic carbon in grasslands with contrasting soil types. Biogeochemistry 91(2):117–131. doi:10.1007/s10533-008-9263-y

Driscoll CT, Mason RP, Chan HM, Jacob DJ, Pirrone N (2013) Mercury as a global pollutant: sources, pathways, and effects. Environ Sci Technol 47 (10):4967–4983. doi:10.1021/es305071v

Eichholz GG, Petelka MF, Kury RL (1988) Migration of elemental mercury through soil from simulated burial sites. Water Res 22 (1):15–20. doi:10.1016/0043-1354(88)90126-1

Futter MN, Poste AE, Butterfield D, Dillon PJ, Whitehead PG, Dastoor AP, Lean DRS (2012) Using the INCA-Hg model of mercury cycling to simulate total and methyl mercury concentrations in forest streams and catchments. Sci Total Environ 424:219–231

Gabriel M, Williamson D (2004) Principal biogeochemical factors affecting the speciation and transport of mercury through the terrestrial environment. Environ Geochem Health 26(3):421–434. doi:10.1007/s10653-004-1308-0

Guédron S, Grangeon S, Jouravel G, Charlet L, Sarret G (2013) Atmospheric mercury incorporation in soils of an area impacted by a chlor-alkali plant (Grenoble, France): contribution of canopy uptake. Sci Total Environ 445–446:356–364. doi:10.1016/j.scitotenv.2012.12.084

Gustafsson JP (1999) WinHumicV For Win95/98/NT. Retrieved from http://www2.lwr.kth.se/English/OurSoftWare/WinHumicV/index.htm

Hylander LD, Meili M (2003) 500 years of mercury production: global annual inventory by region until 2000 and associated emissions. Sci Total Environ 304:13–27

Jacques D, Šimůnek J, Mallants D, Van Genuchten MT (2006) Operator-splitting errors in coupled reactive transport codes for transient variably saturated flow and contaminant transport in layered soil profiles. J Contam Hydrol 88:197–218

Jacques D, Šimůnek J, Mallants D, van Genuchten MT (2008a) Modeling coupled hydrologic and chemical processes: long-term uranium transport following phosphorus fertilization. Vadose Zone J 7(2): 698–711. doi:10.2136/vzj2007.0084

Jacques D, Šimůnek J, Mallants D, Van Genuchten MT (2008b) Modelling coupled water flow, solute transport and geochemical reactions affecting heavy metal migration in a podzol soil. Geoderma 145(3–4):449–461

Jawitz JW, Fure AD, Demmy GG, Berglund S, Rao PSC (2005) Groundwater contaminant flux reduction resulting from nonaqueous phase liquid mass reduction. Water Resour Res 41(10), W10408. doi:10.1029/2004wr003825

Johannesson KH, Neumann K (2013) Geochemical cycling of mercury in a deep, confined aquifer: insights from biogeochemical reactive transport modeling. Geochim Cosmochim Acta 106:25–43. doi:10.1016/j.gca.2012.12.010

Kocman D, Horvat M, Pirrone N, Cinnirella S (2013) Contribution of contaminated sites to the global mercury budget. Environ Res. doi:10.1016/j.envres.2012.12.011

Kothawala DN, Moore TR, Hendershot WH (2008) Adsorption of dissolved organic carbon to mineral soils: a comparison of four isotherm approaches. Geoderma 148(1):43–50

Leterme B, Blanc P, Jacques D (2013) Mercury fate and transport in soil systems—conceptual and mathematical model development and sensitivity study. SNOWMAN Network, enhanced knowledge in mercury fate and transport for improved management of Hg soil contamination

Li Y, Yin Y, Liu G, Cai Y (2012) Advances in speciation analysis of mercury in the environment. In: Liu G, Cai Y, O'Driscoll N (eds) Environmental chemistry and toxicology of mercury. Wiley, New York, pp 15–58. doi:10.1002/9781118146644.ch7

Liu G, Xue W, Tao L, Liu X, Hou J, Wilton M, Gao D, Wang A, Li R (2014) Vertical distribution and mobility of heavy metals in agricultural soils along Jishui River affected by mining in Jiangxi Province, China. Clean Soil Air Water. doi:10.1002/clen.201300668

Mao X, Prommer H, Barry DA, Langevin CD, Panteleit B, Li L (2006) Three-dimensional model for multi-component reactive transport with variable density groundwater flow. Environ Model Softw 21(5):615–628

Massman WJ (1999) Molecular diffusivities of Hg vapor in air, O2 and N2 near STP and the kinematic viscosity and thermal diffusivity of air near STP. Atmos Environ 33(3):453–457

Mayer KU, Frind EO, Blowes DW (2002) Multicomponent reactive transport modeling in variably saturated porous media using a generalized formulation for kinetically controlled reactions. Water Resour Res 38(9):1174. doi:10.1029/2001wr000862

Millan R, Schmid T, Sierra MJ, Carrasco-Gil S, Villadóniga M, Rico C, Ledesma DMS, Puente FJD (2011) Spatial variation of biological and pedological properties in an area affected by a metallurgical mercury plant: Almadenejos (Spain). Appl Geochem 26(2):174–181

Millington RJ, Quirk JP (1961) Permeability of porous solids. Trans Faraday Soc 57:1200–1207. doi:10.1039/tf9615701200

Navarro A, Biester H, Mendoza JL, Cardellach E (2006) Mercury speciation and mobilization in contaminated soils of the Valle del Azogue Hg mine (SE, Spain). Environ Geol 49(8):1089–1101. doi:10.1007/s00254-005-0152-6

Navarro-Flores A, Martínez-Frías J, Font X, Viladevall M (2000) Modelling of modern mercury vapor transport in an ancient hydrothermal system: environmental and geochemical implications. Appl Geochem 15 (3):281–294. doi:10.1016/S0883-2927(99)00046-3

Ottesen RT, Birke M, Finne TE, Gosar M, Locutura J, Reimann C, Tarvainen T (2013) Mercury in European agricultural and grazing land soils. Appl Geochem. doi:10.1016/j.apgeochem.2012.12.013

Pant P, Allen M, Tansel B (2010) Mercury uptake and translocation in Impatiens walleriana plants grown in the contaminated soil from oak ridge. Int J Phytoremediat 13(2):168–176. doi:10.1080/15226510903567489

Parkhurst DL, Appelo CAJ (1999) User's guide to PHREEQC (version 2)—a computer program for speciation, batch-reaction, one-dimensional transport, and inverse geochemical calculations. Vol Water-resources investigations report 99–4259. U.S. Department of the Interior, U.S. Geological Survey, Denver, Colorado, USA

Parkhurst DL, Kipp KL, Charlton SR (2010) PHAST version 2—a program for simulating groundwater flow, solute transport, and multicomponent geochemical reactions. U.S. Geological Survey Techniques and Methods 6-A35

Pérez-Sanz A, Millán R, Sierra MJ, Alarcín R, García P, Gil-Díaz M, Vazquez S, Lobo MC (2012) Mercury uptake by Silene vulgaris grown on contaminated spiked soils. J Environ Manag 95(Supplement):S233–S237. doi:10.1016/j.jenvman.2010.07.018

Powell KJ, Brown PL, Byrne RH, Gajda TS, Hefter G, Sjöberg S, Wanner H (2005) Chemical speciation of environmentally significant heavy metals with inorganic ligands. Part 1: the Hg2+—Cl–, OH–, CO32–, SO42–, and PO43– aqueous systems (IUPAC Technical Report). Pure Appl Chem 77(4):739–800. doi:10.1351/pac200577040739

Prommer H, Barry DA, Zheng C (2003) Modflow/Mt3dms-based reactive multicomponent transport modeling. Ground Water 41(2):247–257. doi:10.1111/j.1745-6584.2003.tb02588.x

Ravichandran M (2004) Interactions between mercury and dissolved organic matter: a review. Chemosphere 55(3):319–331

Renneberg AJ, Dudas MJ (2001) Transformations of elemental mercury to inorganic and organic forms in mercury and hydrocarbon co-contaminated soils. Chemosphere 45(6–7):1103–1109

Rinklebe J, During A, Overesch M, Du Laing G, Wennrich R, Stärk H-J, Mothes S (2010) Dynamics of mercury fluxes and their controlling factors in large Hg-polluted floodplain areas. Environ Pollut 158(1):308–318

Santoro A, Terzano R, Blo G, Fiore S, Mangold S, Ruggiero P (2010) Mercury speciation in the colloidal fraction of a soil polluted by a chlor-alkali plant: a case study in the South of Italy. J Synchrotron Radiat 17 (2):187–192. doi:10.1107/S0909049510002001

Schlüter K (2000) Review: evaporation of mercury from soils. An integration and synthesis of current knowledge. Environ Geol 39(3):249–271. doi:10.1007/s002540050005

Scholtz MT, Van Heyst BJ, Schroeder WH (2003) Modelling of mercury emissions from background soils. Sci Total Environ 304(1–3):185–207

Schuster E (1991) The behavior of mercury in the soil with special emphasis on complexation and adsorption processes—a review of the literature. Water Air Soil Pollut 56:667–680

Sen TK, Khilar KC (2006) Review on subsurface colloids and colloid-associated contaminant transport in saturated porous media. Adv Colloid Interf Sci 119(2–3):71–96

Shaw SA, Al TA, MacQuarrie KTB (2006) Mercury mobility in unsaturated gold mine tailings, Murray Brook mine, New Brunswick, Canada. Appl Geochem 21(11):1986–1998

Šimůnek J, Šejna M, Saito H, Sakai M, van Genuchten MT (2008) The Hydrus-1D software package for simulating the movement of water, heat, and multiple solutes in variably saturated media, version 4.0. Vol HYDRUS software series 3. Department of Environmental Sciences, University of California Riverside, Riverside, California, USA

Šimůnek J, He C, Pang L, Bradford SA (2006) Colloid-facilitated solute transport in variably saturated porous media. Vadose Zone J 5(3):1035–1047. doi:10.2136/vzj2005.0151

Skyllberg U (2008) Competition among thiols and inorganic sulfides and polysulfides for Hg and MeHg in wetland soils and sediments under suboxic conditions: illumination of controversies and implications for MeHg net production. J Geophys Res 113:G00C03. doi:10.1029/2008jg000745

Skyllberg U (2010) Mercury biogeochemistry in soils and sediments. Dev Soil Sci 34

Skyllberg U (2012) Chemical speciation of mercury in soil and sediment. In: Environmental chemistry and toxicology of mercury. Wiley, pp 219–258. doi:10.1002/9781118146644.ch7

Skyllberg U, Qian J, Frech W, Xia K, Bleam WF (2003) Distribution of mercury, methyl mercury and organic sulphur species in soil, soil solution and stream of a boreal forest catchment. Biogeochemistry 64(1):53–76. doi:10.1023/a:1024904502633

Slowey AJ, Rytuba JJ, Brown GE (2005) Speciation of mercury and mode of transport from placer gold mine tailings. Environ Sci Technol 39(6):1547–1554. doi:10.1021/es049113z

Steefel CI (2009) CrunchFlow—software for modeling multicomponent reactive flow and transport. User's manual. Lawrence Berkeley National Laboratory

Steefel CI, DePaolo DJ, Lichtner PC (2005) Reactive transport modeling: an essential tool and a new research approach for the Earth sciences. Earth Planet Sci Lett 240((3–4)):539–558. doi:10.1016/j.epsl.2005.09.017

Stolk AP (2001) Landelijk Meetnet Regenwatersamenstelling - Meetresultaten 1999. Dutch national precipitation chemistry network. Monitoring results for 1999. Rijksinstituut voor Volksgezondheid en Milieu RIVM

Tipping E, Wadsworth RA, Norris DA, Hall JR, Ilyin I (2011) Long-term mercury dynamics in UK soils. Environ Pollut 159(12):3474–3483

Ullrich SM, Tanton TW, Abdrashitova SA (2001) Mercury in the aquatic environment: a review of factors affecting methylation. Crit Rev Environ Sci Technol 31(3):241–293. doi:10.1080/20016491089226

UNEP (2002) Global mercury assessment. Geneva, Switzerland

van Genuchten MT (1980) A closed-form equation for predicting the hydraulic conductivity of unsaturated soils. Soil Sci Soc Am J 44:892–898

Walvoord MA, Andraski BJ, Krabbenhoft DP, Striegl RG (2008) Transport of elemental mercury in the unsaturated zone from a waste disposal site in an arid region. Appl Geochem 23(3):572–583

Waples JS, Nagy KL, Aiken GR, Ryan JN (2005) Dissolution of cinnabar (HgS) in the presence of natural organic matter. Geochim Cosmochim Acta 69(6):1575–1588

Wissmeier L, Barry DA (2010) Implementation of variably saturated flow into PHREEQC for the simulation of biogeochemical reactions in the vadose zone. Environ Model Softw 25(4):526–538. doi:10.1016/j.envsoft.2009.10.001

Yeh G-T, Sun J, Jardine PM, Burgos WD, Fang Y, Li M-H, Siegel MD (2004) HYDROGEOCHEM 5.0: a three-dimensional model of coupled fluid flow, thermal transport, and HYDROGEOCHEMical transport through variably saturated conditions—version 5.0. ORNL/TM-2004/107. U.S. Department of Energy

Zhang H, Lindberg SE, Barnett MO, Vette AF, Gustin MS (2002) Dynamic flux chamber measurement of gaseous mercury emission fluxes over soils. Part 1: simulation of gaseous mercury emissions from soils using a two-resistance exchange interface mode. Atmos Environ 36 (5):835–846. doi:10.1016/S1352-2310(01)00501-5

Zhu J, Sykes JF (2004) Simple screening models of NAPL dissolution in the subsurface. J Contam Hydrol 72(1–4):245–258

Zhu Y, Ma LQ, Gao B, Bonzongo JC, Harris W, Gu B (2012) Transport and interactions of kaolinite and mercury in saturated sand media. J Hazard Mater 213–214:93–99. doi:10.1016/j.jhazmat.2012.01.061